

THE POWER AND PROSPECTS OF FLUORESCENCE MICROSCOPIES AND SPECTROSCOPIES

Xavier Michalet,¹ Achillefs N. Kapanidis,¹ Ted Laurence,¹
Fabien Pinaud,¹ Soeren Doose,¹ Malte Pflughoeft,¹
and Shimon Weiss^{1,2}

¹Department of Chemistry and Biochemistry, ²Department of Physiology, UCLA,
Young Hall, 607 Charles E. Young Drive East, Los Angeles, California 90095;
email: michalet@chem.ucla.edu; kapanidi@chem.ucla.edu; laurence@chem.ucla.edu;
fpinaud@chem.ucla.edu; sdoose@chem.ucla.edu; pflughoe@chem.ucla.edu;
sweiss@chem.ucla.edu

Key Words two-photon, single-molecule, lifetime, polarization, FRET

■ **Abstract** Recent years have witnessed a renaissance of fluorescence microscopy techniques and applications, from live-animal multiphoton confocal microscopy to single-molecule fluorescence spectroscopy and imaging in living cells. These achievements have been made possible not so much because of improvements in microscope design, but rather because of development of new detectors, accessible continuous wave and pulsed laser sources, sophisticated multiparameter analysis on one hand, and the development of new probes and labeling chemistries on the other. This review tracks the lineage of ideas and the evolution of thinking that have led to the actual developments, and presents a comprehensive overview of the field, with emphasis put on our laboratory's interest in single-molecule microscopy and spectroscopy.

CONTENTS

INTRODUCTION	162
FUNDAMENTALS OF FLUORESCENCE, FLUOROPHORES AND LABELING, AND FLUORESCENCE DETECTION	163
Fundamentals of Fluorescence	163
Fluorophores and Labeling	166
Fluorescence Detection	167
FLUORESCENCE IMAGING: A CLASSIC REVISITED	168
Imaging Modes: Intensity, Spectrum	168
Other Imaging Modes: Lifetime, Time-Gated, and FRET Imaging	169
High-Resolution Imaging and Localization	170
SINGLE-MOLECULE SENSITIVITY: WATCHING MOLECULES ROCK 'N ROLL	171
Signal-to-Noise Requirement	171

The Signature of a Single Fluorophore	172
Single-Molecule Fluorescence Observation	173
CONCLUSION	175

INTRODUCTION

Optical microscopy has made continuous progress since it was born at the end of the sixteenth century, with the creation of the first two-lens microscope by the Jansens in Middleburg, Holland. Today's research microscopes and objective lenses have been perfected to achieve the diffraction limit of resolution defined by Ernst Abbe at the end of the nineteenth century (1). Since this landmark, advances in (nonfluorescence) optical microscopy have come from new imaging modes such as phase contrast, Nomarski's differential interference contrast (DIC), or Hoffman's contrast, to name a few. Despite their advantages in enhancing contrast or details due to variations in the index of refraction, these transmitted-light techniques do not provide any means to distinguish individual objects or identify small organelles other than by their shape or optical density. To circumvent this limitation, staining agents and techniques have been developed by histologists since the beginning of microscopy. However colorful, these techniques developed before the advent of molecular biology have staining specificities that rely on poorly understood interactions. They also do not allow the detection of objects that are smaller than the diffraction limit or that do not present enough contrast. Fluorescence microscopy overcomes these limitations by rejecting the excitation light, leaving visible only the sources of emission. The development of immunocytochemistry during the twentieth century gave this technique its full potential. Initially limited to fixed samples, fluorescence immunocytochemistry was extended to live cell imaging during the 1980s (133).

Confocal laser scanning microscopy (CLSM) has also steadily grown as an indispensable tool for three-dimensional imaging. CLSM capabilities have been extended to include multiphoton excitation processes and lifetime imaging, or to improve its three-dimensional resolution. Progress in detector technology, interest in the photophysics of single-quantum emitters, and questions arising from the burgeoning field of single-molecule biophysics have recently pushed fluorescence microscopy to its ultimate level of sensitivity. Single fluorescent molecules can now be detected in a living cell and localized with nanometer precision in real time. In parallel with these improvements in image versatility, sensitivity, and resolution, fluorescence has also been used as a tool to probe the dynamics, conformational changes, and interactions of single molecules. This modern development has completed the transition of fluorescence microscopy from a purely imaging technique to nanospectroscopy (spectroscopy of small volumes), extending the application of the microscope to structural biology, biochemistry, and biophysics, and providing new tools for the postgenomic (i.e., proteomic) era. Single-molecule spectroscopy (SMS) has recently shed light on inter- and intramolecular interactions,

protein folding, and protein structure, as well as on the functioning of the cellular machinery.

This article gives an overview of achievements in the field of fluorescence microscopy and spectroscopy, as well as reviews recent developments focused on single-molecule sensitivity. As they take full advantage of the properties of the fluorescence emission process by individual molecules, we first present in some detail experimental results illustrating each of these properties. We then discuss how to practically take advantage of these capabilities by presenting an overview of fluorescent labeling techniques and experimental setups. The two final parts review imaging applications of fluorescence and single-molecule experiments.

FUNDAMENTALS OF FLUORESCENCE, FLUOROPHORES AND LABELING, AND FLUORESCENCE DETECTION

Fundamentals of Fluorescence

Fluorescence is the phenomenon of photon emission following absorption of one (or more) photon(s) by a molecule or material (fluorophore) that returns to its ground state. First observed for quinine by Herschel in the early nineteenth century, it was further studied by Stokes who correctly identified its main characteristics (for the case of single-photon excitation), namely that the emitted photons have a longer wavelength than the absorbed ones (70). A series of experimental and theoretical studies by several investigators in the early twentieth century uncovered most of today's known properties of fluorescence (99).

Excitation and emission processes in a typical molecule are represented by a Jablonski diagram (Figure 1) depicting the initial, final, and intermediate electronic and vibrational states of the molecule. In general, fast intramolecular vibrational relaxations result in emitted photons having a lower energy than do the incident ones (or equivalently, a larger wavelength, the difference being the so-called Stokes shift). This property is the basis of the simple separation of emitted fluorescence from excitation light, which renders fluorescence such a powerful tool. The emitted photon is detected within a typical delay (lifetime) after absorption of the excitation photon, which depends on the species studied and its local environment. Organic dyes have typical lifetimes from several tens of picoseconds to several nanoseconds. Longer lifetimes are obtained for fluorescent semiconductor nanocrystals (NCs) (tens of ns), organometallic compounds (hundreds of ns), and lanthanide complexes (up to ms). The probability distribution of emission times is usually monoexponential, characterized by a lifetime $\tau = \Gamma^{-1} = (k_r + k_{nr})^{-1}$, where k_r and k_{nr} are the radiative and nonradiative decay rates, respectively (Figure 1). The latter is dependent on the local environment via perturbations of the intramolecular transition matrix elements. For instance, the proximity to a dielectric or metallic surface markedly modifies the fluorescence lifetime (6, 141).

While in its excited state, a molecule has a probability to end up in a nonemitting triplet-state during microseconds to milliseconds, resulting in dark states (52, 95).

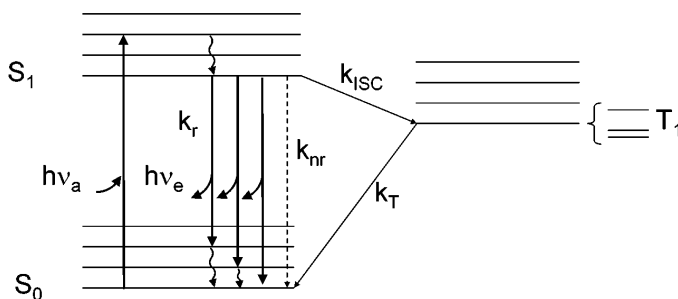


Figure 1 Jablonski diagram for fluorescence. Upon absorption of a photon of energy $h\nu_a$ close to the resonance energy $E_{S_1} - E_{S_0}$, a molecule in a vibronic sublevel of the ground singlet state S_0 is promoted to a vibronic sublevel of the lowest excited singlet state S_1 . Nonradiative, fast relaxation brings the molecule down to the lowest S_1 sublevel in picoseconds. Emission of a photon of energy $h\nu_e < h\nu_a$ (radiative rate k_r) can take place within nanoseconds and bring back the molecule to one of the vibronic sublevels of the ground state. Alternatively, collisional quenching may bring the molecule back to its ground state without photon emission (nonradiative rate k_{nr}). A third type of process present in organic dye molecules is intersystem crossing to the first excited triplet state T_1 (rate k_{ISC}). Relaxation from this excited state back to the ground state is spin-forbidden, and thus the lifetime of this state is in the order of microseconds to milliseconds. Relaxation to the ground state takes place either by photon emission (phosphorescence) or nonradiative relaxation. The fluorescence lifetime is defined by $\tau = 1/\Gamma = (k_r + k_{nr})^{-1}$.

Other fluorescent molecules such as green fluorescent proteins (GFPs) (31) or semiconductor NCs (37) exhibit similar dark state intervals, although for different reasons [different long-lived dark states for GFP (31), Auger ionization or surface trapping of carriers for NC (35)].

Spectral jumps can also be observed at the single-molecule level (53). This phenomenon results from a shift of absorption and emission maxima due to the changing environment of the molecule or a sudden conformational change of the molecule itself (5, 125, 141).

The efficiency of photon absorption is proportional to $(\vec{E} \cdot \vec{\mu})^2$, where \vec{E} represents the local electric field, and $\vec{\mu}$ is the absorption dipole moment of the fluorophore (55, 70). For an immobilized fluorophore, the orientation of the molecule's absorption dipole can thus be determined by recording the emitted fluorescence as a function of the orientation of the linear polarization of the excitation light. This information in turn allows the determination of the spatial orientation of the fluorophore (51, 141). For a mobile molecule, more information is needed because the emission dipole may have time to tumble significantly (54): Fluctuations faster than the fluorescence lifetime lead to a depolarized emission; fluctuations taking place over timescales longer than the lifetime but shorter than the integration time

lead to anticorrelation of the two orthogonal emission polarizations. The emission polarization is needed to fully recover the relevant information. In particular, it is important to recover the projection of the polarization on more than two orthogonal axes as illustrated in Figure 2. This can be achieved in different ways in wide-field imaging approaches as well as confocal ones (39).

Fluorescence resonance energy transfer (FRET), first described theoretically by Perrin (100) and later fully elucidated by Förster (40), is a special case of influence of the local environment on fluorescence. If a nearby molecule (acceptor) has an absorption spectrum overlapping with the emission spectrum of the studied molecule (donor), the energy absorbed by the donor can be transferred

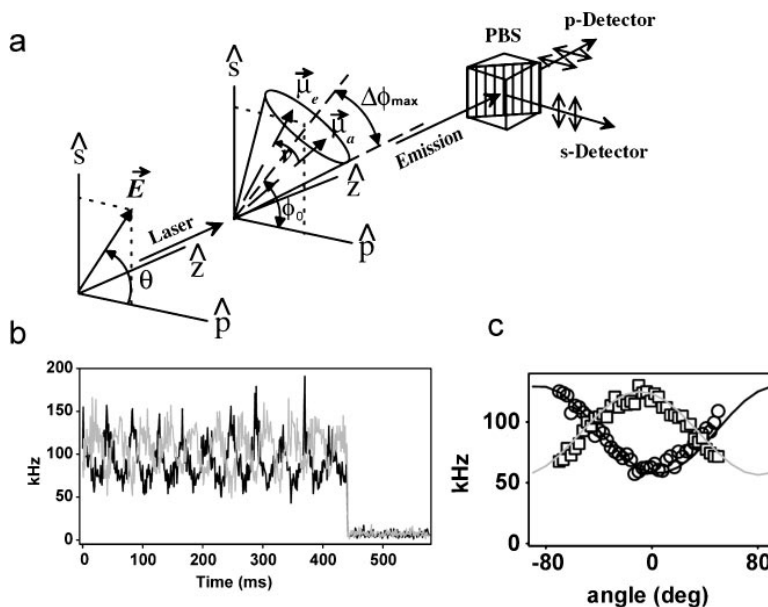


Figure 2 (a) Experiment schematic. \vec{E} : electric field, making an angle θ with the p polarization axis. The excitation propagates along axis z , which is also the collection axis. $\vec{\mu}_a$ and $\vec{\mu}_e$ are the absorption and emission dipole moments, initially aligned. ν represents the rotational diffusion of the emission dipole during the excited lifetime. The dipole is supposed to be confined in a cone positioned at an angle ϕ_0 projected on the (s, p) plane that has a half-angle $\Delta\phi_{\max}$. A polarizing beam-splitter (PBS) splits the collected emission in two signals I_s and I_p , which are simultaneously recorded by APDs. (b) Simultaneously recorded I_s (black) and I_p (gray) of a molecule rapidly rotating in liquid. (c) Same data as in (b), but average over the 11 “on” periods. The fit corresponds to a $\Delta\phi_{\max}$ close to 90° (freely rotating molecule) and permits determination of the constrained rotational diffusion parameter. Adapted with permission from Reference 54. Copyright 1998, the American Physical Society.

nonradiatively to the acceptor with an efficiency E given by:

$$E = \left(1 + (r/R_0)^6\right)^{-1}, \quad 1.$$

where r is the distance between the two emitting centers, and R_0 is the Förster radius (in Å). R_0 is of the order of a few nanometers. Stryer & Haugland (118) thus suggested using it as a molecular ruler. An example of this utilization is given in Figure 3. The corresponding donor-acceptor distances are measured on diffusing molecules with subnanometer precision, using the relative intensities in each color channel. Alternatively, the transfer efficiency can be measured via the fluorescence lifetimes as: $E = 1 - \tau_{D(A)}/\tau_{D(0)}$, where $\tau_{D(A)}$ and $\tau_{D(0)}$ are the donor lifetimes in the presence or absence of acceptor, respectively (49). Electron transfer can also significantly perturb the lifetime of a dye by opening a new nonradiative path in the Jablonski diagram of the molecule (Figure 1).

Although most single-molecule experiments use one-photon fluorescence excitation because of its relatively large cross-section ($\sim 10^{-16}$ cm²), fluorescence can also be excited via a two-photon absorption process (28) using laser excitation with half the photon energy needed to attain the excited state (106). However, because of the low cross-section and the quadratic dependence on the incident power, an excitation power several orders of magnitude larger than for one-photon excitation is needed. This increases photobleaching because of the high probability of photochemical degradation in the long-lived triplet state and the interplay of multiphoton ionization processes (32). In compensation, excitation takes place in a substantially reduced volume of the sample, reducing the out-of-focus background contribution and out-of-focus bleaching.

Fluorophores and Labeling

A great variety of fluorophores are available (59, 70). Fluorescent organic molecules (13), GFPs (31) and other fluorescent proteins (73), conjugated polymers (J-aggregates) (130), light-harvesting complexes (140), dendrimers (62), or semiconductor NCs (37) are a few examples of systems that have been extensively studied at cryogenic as well as at room temperature with SMS techniques. Each of these systems exhibits fluorescence based on specific processes, which can be quite different from that illustrated on Figure 1. In NCs (4) for instance, ultraviolet-visible photon absorption by a semiconductor compound leads to the creation of an electron-hole pair (exciton). The pair recombines within few tens of nanoseconds, emitting a visible photon whose wavelength depends on the NC diameter owing to quantum confinement effects (4).

Fluorophores can be added *in vitro* to most proteins or other biomolecules after biosynthesis and purification (132), either statistically or specifically. Statistical labeling is mainly used for imaging purposes or restricted to preliminary stages of assay development, as for the FRET-based analysis of staphylococcal nuclease dynamics (56). However, site-specific labeling is a necessity when precise distance or orientation information is sought (27). It requires a careful choice of labeling

TABLE 1 Labeling strategies

Method	Application	References
Cysteine-specific labeling with thiol-reactive reagents	Widespread use for FRET and fluorescence polarization analysis of small proteins (<500 residues)	(2, 42, 59, 68, 107, 112, 127, 132, 135)
Bis-functional Cys-reactive fluorophore	Monitoring of orientation and dynamics of protein domains	(20, 101, 116)
Peptide ligation	Intramolecular FRET	(21, 24, 27, 88, 113, 122)
Fluorescent derivatives of the antibiotic puromycin	C terminus labeling	(90, 143)
In vitro reconstitution from purified components	Multicomponent complexes	(80, 89, 107, 135)
Genetically encoded fluorescent protein	In vivo labeling	(48, 63, 126)

chemistry, optimization of labeling reaction, and rigorous characterization of the labeled biomolecules for efficiency, site-specificity, and retention of functionality. Some of the many available methods, which are discussed in detail in (66), are presented in Table 1. Few molecules do not require labeling because of the presence of fluorescent moieties either in their own structure or in cofactors. This is the case of proteins with tryptophan residues, enzymes using NADH, or flavins as cofactors, as illustrated in Reference 73. This autofluorescence of native proteins is in fact a source of background in cell fluorescent imaging applications.

Fluorescence Detection

Fluorescence acquisition geometries can be classified according to their excitation and emission schemes. Wide-field detection schemes use either epifluorescence illumination with lamps (47), defocused laser excitation (109), or total internal reflection (TIR) excitation (42). Detectors include back-thinned charge-coupled devices (CCDs) with quantum efficiencies (QE) up to 90%, but a usable readout rate limited by readout noise to a few full frames per second (47, 109). Intensified CCDs overcome the readout noise limitation by signal amplification, allowing higher frame rates but at the price of a lower QE (<40%). The new electron-multiplying CCD technology should permit increased frame rates, with transfer rates as high as 10 MPixels/s with single-molecule sensitivity (74).

Point-detection schemes encompass confocal and near-field scanning optical microscopies (NSOM). The excitation volume has a radius of the order of the excitation wavelength for CLSM (97) and of the tapered fiber core (~100 nm) for NSOM (Figure 4) (14, 38). Images of the sample are acquired pixel by pixel in a raster fashion using a point-detector and reconstructed by software.

Commercial CLSM uses a pair of galvanometer-mounted mirrors or acousto-optical deflectors to move the excitation laser beam across the sample and photomultiplier tubes (PMT) for photon detection. This choice has the advantage of great speed (video-rate imaging is possible) but does not provide enough sensitivity for SMS. SMS requires a slower, stage-scanning method and sensitive avalanche photodiodes (APD). Indeed, until recently, PMT had a QE <20% in the visible spectrum, against ~70% for silicon APD. Progress in photocathode technology (using GaAsP) should increase the QE of PMT, making them attractive detectors for beam-scanning CLSM because of their larger sensitive area.

In one version of NSOM that closely resembles the original suggestion by Syngge (119) at the beginning of the twentieth century, a narrow optical fiber is brought in close proximity (tens of nm) to a sample and a raster is scanned over it (25). The underlying molecules are sensitive only to the near-field contribution of the transmitted laser electric field, which extends over distances smaller than the wavelength, resulting in a higher-resolution image collected by a microscope objective lens (38).

The use of lasers as excitation sources limits the range of accessible excitation wavelengths but provides higher intensities and allows pulsed excitation with ultrafast lasers. They can be used in the near-infrared (NIR) range to perform two-photon fluorescence excitation, whose square dependence on the intensity results in a quick decrease of the excitation away from the focus (28). Even though spatial resolution is not necessarily enhanced and fluorophore photobleaching is increased (96), two advantages result from this rather expensive and still sophisticated technique: Out-of-focus bleaching is reduced, and sample penetration is increased because of the reduced absorption of NIR radiation, allowing thick, live tissues to be imaged with little damage to the environment. The technique has thus found impressive applications in neuroimaging (77) and deep-tissue imaging (114).

In SMS, wide-field imaging is necessary for particle-tracking studies but can also be preferred over single-point detection for simultaneous observation of several spatially separated molecules (109). This reduces the amount of time needed to accumulate a statistically significant number of observations. It is especially relevant for experiments in which irreversible processes are triggered by modification of an external parameter. Point-detection geometries allow the acquisition of fluorescence time traces of immobilized molecules with high temporal resolution, as well as fluorescence lifetime information (75), but they are rather slow for imaging single molecules. CLSM is also extensively used for the study of freely diffusing molecules in solution or embedded in fluid membrane (lipid bilayer of cell membranes) by fluorescence correlation spectroscopy (FCS) (111, 139).

FLUORESCENCE IMAGING: A CLASSIC REVISITED

Imaging Modes: Intensity, Spectrum

Fluorescence allows rejection of the excitation signal and only detection of the fainter emission light using filters and dichroic mirrors. This does not lead to any

resolution improvement, but subresolution objects can now be detected as contrasted spots of fluorescent light with a diffraction-limited size (the point spread function, or PSF). With the advent of digital, high-sensitivity cameras, successive excitation and detection of different fluorophores make it possible to obtain multicolor images with good signal-to-noise ratio (SNR) (61).

Standard fluorophores have broad-emission spectra, a fact that renders their spectral separation by bandpass interference filters imperfect, and impractical in the case of several colors. It is then advantageous to use spectral imaging methods that collect all emitted light for further processing. Several of these methods have been proposed and implemented in recent years, both in wide-field (78) and point-detection geometries (30, 69). Their goal is to recover the contribution of each fluorophore to the recorded emission at different wavelengths for each individual pixel. Fluorescence being an incoherent process and emission spectra being well defined, intensities from different fluorophores simply add at each wavelength of the emission spectrum. Knowing the emission spectra, we can recover the contribution of each individual fluorophore by a simple matrix inversion. Figure 5 illustrates this point with a mixture of five semiconductor NC samples spin-coated on a cover-glass and imaged with a prism and ICCD-based confocal spectrometer (69, 82). These and future developments may improve the sensitivity of ion- or pH-sensitive fluorophores (59), which are characterized by spectral changes upon variation of the local concentration of an ionic species and have been used at the single-molecule level (17).

Other Imaging Modes: Lifetime, Time-Gated, and FRET Imaging

After intensity and spectrum, fluorescence lifetime is the next most useful observable fluorescence emission property for imaging. Most fluorophores excited by a pulsed laser emit fluorescence photons after a few nanoseconds. Lifetime is extremely sensitive to the molecule's environment. The purpose of fluorescence lifetime imaging (FLIM) is thus to measure the fluorescence lifetime at each point of a sample to map either the presence or absence of a species, or the environment of a known single fluorophore (45, 134). This is especially relevant for fluorescent proteins such as GFP, which cannot easily be separated spectrally (98). Two implementations of this technique are available: One uses a time-domain measurement (124), the other a frequency-domain measurement (45, 71, 134). The time-domain approach can be implemented using a time-correlated single-photon counting (TCSPC) confocal setup (124), or using a time-gated ICCD in either a multifoci excitation configuration (117) or a wide-field illumination (11). In the first case, the scanning process is time-consuming, while in the second the camera detects only photons emitted during a fixed time-window after the laser pulse, losing any information on the remaining photons. In particular, time-gated detection can only distinguish between fluorophores of well-separated lifetimes and necessitates acquiring two sets of images for that purpose. This technique has

been exploited for lanthanide chelates (131), metal ligand complexes (123), and NC (22) imaging. These fluorophores have much longer lifetimes than do the autofluorescence of cell proteins, which make them attractive probes for high-sensitivity, background-free intracellular imaging (Figure 6).

The frequency-domain approach is no less complicated and is based on radio-frequency (RF) modulation of the laser intensity and of the image intensifier gain, either in phase (homodyne) or out-of-phase (heterodyne). The acquisition of several images at different phase differences allows the calculation of an apparent lifetime and concentration for each pixel of the image, but this process can be extremely time-consuming (several minutes) (72), resulting in photobleaching. Applications to live intracellular Ca^{2+} imaging (72) or of receptor phosphorylation events (92) have illustrated the power of this imaging technique where spectral information is of little help. The advantages of two-photon microscopy can be combined with FLIM in the frequency domain (102, 115), time-gated FLIM (120), or TCSPC FLIM (10).

FRET imaging was first explored using fluorescence donor/acceptor photobleaching (23, 44) in order to extract background components of the signal. However, the irreversible modification of the sample that follows makes it far from ideal. Other methods have been proposed. FLIM can measure energy transfer using the relation $E = 1 - \tau_{D(A)}/\tau_{D(0)}$ introduced previously. It provides a concentration-independent FRET measurement and minimizes illumination (43). A combination of intensity and lifetime observations would benefit FRET study (57), giving access to dynamic interactions between FRET pairs on a cell-wide scale.

High-Resolution Imaging and Localization

Compared to an optical-sectioning technique such as DIC, standard fluorescence microscopy suffers from image blurring due to out-of-focus signal. Deconvolution algorithms have been developed during the 1980s in order to reassign out-of-focus light back to its original source location, using series of images taken at different foci (3). The reliability and ease of use of these algorithms have improved steadily with computer power, allowing in certain conditions imaging with a resolution better than the diffraction limit (super resolution) (18). Still, limited image transfer rate and processing time confine these techniques to fixed samples or slow processes. CLSM has come as a remedy to blurring by removing most ray-lights emitted out of focus with a pinhole (97).

Nevertheless, the resolution is still limited by the extension of the excitation PSF. Working toward reducing the excitation volume, several PSF engineering strategies have been proposed and demonstrated in order to reduce it at least in one direction. Interference methods have been implemented that create a narrower central excitation volume along the optical axis thus improving the vertical resolution of fluorescence microscopy (8, 41, 50, 60). A more sophisticated approach, stimulated emission depletion (STED), takes full advantage of the physics of fluorescence emission (67). Combining both approaches, an image with a

three-dimensional resolution of ~ 30 nm has recently been obtained (33). This imaging resolution is close to the best performances of NSOM and is not limited to surface studies.

Although improvements in imaging resolution are still possible, a much better performance has already been reported in a related problem: high-resolution (co)localization. In this case, one is interested not so much in the exact geometric structure of an object than in the relative position of two objects. This problem has been investigated thoroughly in the domain of bright-field microscopy, where micrometer-sized beads were observed and localized with nanometer resolution using centroid-finding algorithms (46). In fluorescence microscopy, the image is that of the PSF. If it is detailed enough and if its SNR is large enough, precise subpixel localization can be obtained (12, 15). This idea has been successfully put in practice at the single-molecule level in near-field (53), wide-field (109, 110), and confocal microscopy (69). Reaching nanometer resolution requires a careful consideration of all sources of optical aberrations, especially chromatic if one considers distances between objects with different colors. For these reasons, NCs, which can all be excited by a single visible wavelength and detected simultaneously, represent in principle the ultimate probe for this type of application (Figure 7) (69, 81).

SINGLE-MOLECULE SENSITIVITY: WATCHING MOLECULES ROCK 'N ROLL

The field of SMS has rapidly grown since its inception in the 1990s. The ability to watch one molecule at a time gives access to the distribution functions of observables instead of the first statistical moments obtained in ensemble measurements. It helps resolve subpopulations in heterogeneous samples or record asynchronous time trajectories of observables that would otherwise be hidden during biochemical reactions or similar processes.

SMS and microscopy experiments have already been evoked in the first parts of this article to illustrate different properties of fluorescence (Figure 2). We now point to the specific requirements needed to reach single-molecule sensitivity and present a brief overview of applications and prospects of this fast-developing methodology.

Signal-to-Noise Requirement

Single-molecule observations require a careful optimization of background, signal, and noise (83). SNR and signal-to-background ratio (SBR) can be increased by improving the collection efficiency, and the SBR can be further improved by decreasing the excitation volume V . A larger excitation power or a longer integration time improves the SNR without affecting the SBR. The value of the residual background rate can be reduced by a careful choice of buffer, embedding matrix or immersion medium, and rejection filter or use of a confocal design.

For instance, typical values of the relevant parameters in the case of a CLSM study of freely diffusing fluorescein isothiocyanate (FITC) in water may lead to count rates of a few tens to hundreds of counts/ms and SNR ~ 10 (83). However, single molecules have a finite life span. In an oxygen-rich environment, they typically emit on the order of 10^6 photons before irreversible photobleaching. This happens after a few hundred milliseconds, larger than the typical transit time (a few hundred μs). For an immobilized molecule, however, it sets a stringent limit on the total duration of a single-molecule observation.

The Signature of a Single Fluorophore

In addition to SBR and SNR issues, care has to be taken to ensure that the collected signal originates from a single molecule. Several fluorescent molecules can indeed occupy the diffraction-limited excitation volume. If intensity fluctuations (or variations of any other spectroscopic characteristics) are observed, they could be due to single-molecule dynamics or environment changes, but they could as well reflect the stochastic mixture of emissions from nearby molecules.

Two different strategies can be envisioned to reduce this uncertainty: (a) Work at low concentration, such that at most one molecule is present in the excitation volume, or equivalently, minimizes the excitation volume; and (b) use a selective excitation or emission-detection protocol, such that only one molecule is excited or detected within the sampled volume.

The first can be used in both solution and immobilized conditions. The second strategy requires fluorophores having either separable excitation (86, 95) or emission properties (69, 124, 128) and has been illustrated with fluorescent semiconductor NCs in Figure 5.

In addition to fulfilling the above experimental criteria for single-molecule detection, a number of tests can be performed to ascertain that the observed signal actually comes from a single emitter (13). These criteria are direct consequences of the photophysical properties of fluorophores:

- The observed density of emitters varies according to the known concentration of molecules.
- The observed fluorescence intensity level is consistent with that of a single emitting molecule.
- Each immobilized emitter has a well-defined absorption or emission dipole.
- Fluorescence emission exhibits only two levels (on/off behavior due to blinking or photobleaching) over timescales where no changes in the environment are expected (93).
- If there are two or more emission levels, photophysical property changes are correlated (91).
- The emitted light exhibits antibunching, i.e., no simultaneous emission of two photons (9).

Single-Molecule Fluorescence Observation

Single-molecule fluorescence detection has undergone rapid developments in the past few years, spreading in multiple fields of science (64, 83, 85, 136, 137, 142). Here we present only a few examples of its power, with FCS methods, and studies in material science and biology.

FLUORESCENCE CORRELATION SPECTROSCOPY FCS was introduced in the early 1970s (36, 76) as a method to study thermodynamic fluctuations of freely diffusing molecules at the small ensemble level (few molecules diffusing simultaneously within the excitation volume). The method is usually implemented in a confocal detection geometry and involves the recording of the arrival time of all photons emitted in the small detection volume (~ 1 fl). Analysis of the correlation function of the recorded intensity permits extraction of the concentration, diffusion coefficient, photophysical characteristics, and for some of its variants, brightness of one or multiple fluorophores in solution or in fluid membranes (111). The auto-correlation function of a single-channel intensity or the cross-correlation function of multiple channels give access to fast timescales (as well as slower timescales), which are not accessible from the study of individual immobilized molecules due to shot-noise. Simultaneous consideration of other dimensions of fluorescence (polarization, lifetime) or data analysis schemes taking full advantage of the recorded arrival times have given rise to a number of applications in photophysics (138), conformational dynamics (16), macromolecular interactions (104), and study of the kinetics of enzyme-catalyzed reactions (103). Many of the recent developments in detection of molecular interactions have been focused on increasing the sensitivity to brightness to monitor ligand-protein binding equilibria (19), probe the stoichiometry of protein complexes (79), study oligonucleotide-polymer interactions (129), or to probe receptor-ligand interactions in a format compatible with ultrahigh-throughput screening (104, 108). These methods show improved sensitivity over FCS methods that rely on diffusion only.

For interactions between macromolecules of different types (for example heterodimerization of two proteins), extending the analysis to two channels improves the sensitivity over one-channel analysis. The molecules of one type are labeled with one color (e.g., yellow), and the molecules of the other type are labeled with another color (e.g., red). A complex of the two types of molecules thus has both labels. Signal from the two fluorophores is separated spectrally onto two detector channels, yellow and red. The binding of two molecules labeled with the yellow and red fluorophores is indicated by the coincident detection of simultaneous photon bursts on both channels [these applications are reviewed in (103)]. The cross-correlation technique has recently been applied in conjunction with CLSM to cellular environments (7). By imaging and subsequent placement of the confocal spot at a specific point in the cell, the endocytic pathway of bacterial cholera toxin was followed using cross-correlation analysis. Two subunits of the toxin were labeled with different fluorophores, and the subunits were colocalized until

reaching the Golgi apparatus, where they separated. This study demonstrates the potential of cross-correlation analysis in living cells.

MATERIAL SCIENCE STUDIES Single-molecule photophysical properties are extremely sensitive to their local (nanometer-sized) environment (84, 87). They can for instance report on parameters such as the local pH (17) or on the local structure, as illustrated by experiments designed to study the local dynamics of a polymer matrix at the onset of the glass transition (29).

In this later experiment, molecules of the organic fluorophore Rhodamine 6G dispersed within a thin poly(methacrylate) film were observed at temperatures slightly above the melting temperature of the polymer, using fluorescence polarization CLSM (29). Each molecule exhibited a slow rotational diffusion over several hours. This study demonstrated that an individual molecule probes an increasing number of different environments over time (dynamic disorder). At long timescales, the observable characteristics (such as the autocorrelation function) are similar to those measured on an ensemble of molecules, as expected from the ergodicity hypothesis. At short timescales, each molecule reveals the peculiar local and stable characteristic of its nanoenvironment, which may be different from that of another molecule situated elsewhere (static disorder).

BIOPHYSICAL AND BIOLOGICAL STUDIES SMS has allowed a reassessment of long-standing questions in biophysics, biochemistry, and biology (64, 136) by giving scientists the possibility to study conformational dynamics and interactions of individual molecules in biological processes. From simple model systems based on DNA (54, 55) or small peptides (65), to ribozyme (145), motor-proteins (94, 116), and other biomolecules (2), or biomolecular complexes formed by association of a few molecules (121), SMS continues to contribute valuable information to biology.

An example of this versatility is provided by the labeling of the central part of a rotary motor protein, F_1 -ATPase (2). In this experiment, the molecular rotor was labeled with a single fluorophore whose orientation, detected by emission polarization measurements, directly reported the angle of the rotor with respect to the shaft. The small size of the fluorophore guaranteed that the protein motion would not be hindered (contrary to previous experiments, which used many larger reporters such as micron-sized latex beads or fluorescent actin filaments). This experiment (2) reproduced the previous results, showing that the rotor performed 120° steps [more recent work revealed substeps of 90° and 30° (144)].

SMS is also the tool of choice to study protein folding (137). The transition from a denatured state to the fully folded native protein usually involves an unknown number of intermediate states, which are not accessible by ensemble measurements. Conformations of doubly labeled proteins can be monitored by SMS as they undergo folding, taking advantage of the distance dependence of FRET (Figure 3). Our laboratory has studied the enzyme chymotrypsin inhibitor 2 (CI2), believed to have two clearly distinct folding states. Their equilibrium is controlled by the concentration of denaturant guanidinium chloride (27). Using single-pair FRET

(spFRET) techniques, it was possible to identify folded and unfolded molecules present at different denaturant concentrations. When averaged, these measurements yield the same denaturation curve obtained by ensemble measurements and give access to the energy landscape of the folding reaction. The additional information provided by spFRET is the number of molecules in the two different states, providing direct evidence of the two-states model derived indirectly from ensemble measurements.

Other biological systems have been successfully studied using spFRET on immobilized molecules: spFRET has revealed transient intermediate states in the *Tetrahymena* ribozyme (145), which had remained unnoticed in ensemble studies. In vivo, intermolecular spFRET permits the detection of association and dissociation events, as in the case of an epidermal growth factor receptor pair studied on cell membrane using TIR (105). For cluster formation involving larger numbers of monomers, observed with E-cadherin (63) or L-type Ca^{2+} channels (58), stoichiometric approaches relying on the quantized emission of single molecules can estimate the number of components in an aggregate.

CONCLUSION

Fluorescence microscopy is a mature field that keeps evolving toward higher sensitivity, versatility, and temporal, spectral, and spatial resolution. Its latest developments now allow reaching the level of the single molecule. In the near future, the principal limitations of SMS (low signal, limited lifespan of fluorophores, trade-off between time resolution, and the level of detail of information) will probably remain, but technical improvements toward simultaneous acquisition of all fluorescence parameters (intensity, spectrum, lifetime, polarization) are promising. New detectors will permit the combination of the high time resolution of single-photon counting devices with the large field of view and spectral resolution allowed by two-dimensional detectors. Progress is to be expected in the development of new fluorophores or in their use to probe local environmental properties.

As powerful as it is, SMS cannot replace every existing single-molecule detection or manipulation technique. Researchers start associating it with other approaches to correlate applied forces or fields and molecular conformations. New ways of controlling local fields (electric, magnetic, or others) or biochemical environments (microfluidic devices) would take advantage of the noninvasiveness, high-temporal, and spatial resolution of SMS to get a direct feedback of events at the nanometer scale in various domains of research. We thus expect that it will be possible to follow biological processes at the molecular level in individual cells.

ACKNOWLEDGMENTS

Contributions of actual and former members of the laboratory to the development of SMS and microscopy are gratefully acknowledged. Part of the work described here has been supported by NIH National Center for Research Resources grant

7 R01 RR14891-02, NIH National Institute of General Medical Sciences grant 1 R01 GM65382-01, and DOE grant DE-FG03-02ER63339.

**The Annual Review of Biophysics and Biomolecular Structure is online at
<http://biophys.annualreviews.org>**

LITERATURE CITED

1. Abbe E. 1873. Beiträge zur Theorie der Mikroskops und der mikroskopischen Wahrnehmung. *Schultze Arch. Mikrosk.* 9: 413–68
2. Adachi K, Yasuda R, Noji H, Itoh H, Harada Y, et al. 2000. Stepping rotation of F1-ATPase visualized through angle-resolved single-fluorophore imaging. *Proc. Natl. Acad. Sci. USA* 97:7243–47
3. Agard DA, Sedat JW. 1983. Three-dimensional architecture of a polytene nucleus. *Nature* 302:676–81
4. Alivisatos AP. 1996. Semiconductor clusters, nanocrystals, and quantum dots. *Science* 271:933–37
5. Ambrose WP, Moerner WE. 1991. Fluorescence spectroscopy and spectral diffusion of single impurity molecules in a crystal. *Nature* 349:225–27
6. Ambrose WP, Goodwin PM, Martin JC, Keller RA. 1994. Alterations of single molecule fluorescence lifetimes in near-field optical microscopy. *Science* 265:364–67
7. Bacia K, Majoul IV, Schwille P. 2002. Probing the endocytic pathway in live cells using dual-color fluorescence cross-correlation analysis. *Biophys. J.* 83:1184–93
8. Bailey B, Farkas DL, Taylor DL, Lanni F. 1993. Enhancement of axial resolution in fluorescence microscopy by standing-wave excitation. *Nature* 366:44–48
9. Basché T, Moerner WE, Orrit M, Talon H. 1992. Photon antibunching in the fluorescence of a single dye molecule trapped in a solid. *Phys. Rev. Lett.* 69:1516–19
10. Becker W, Bergmann A, König K, Tirlapur U. 2001. Picosecond fluorescence lifetime microscopy by TCSPC imaging. *Proc. SPIE* 4262:414–19
11. Beeby A, Botchway SW, Clarkson IM, Faulkner S, Parker AW, et al. 2000. Luminescence imaging microscopy and lifetime mapping using kinetically stable lanthanide(III) complexes. *J. Photochem. Photobiol. B* 57:83–89
12. Betzig E. 1995. Proposed method for molecular optical imaging. *Opt. Lett.* 20: 237–39
13. Betzig E, Chichester RJ. 1993. Single molecules observed by near-field scanning optical microscopy. *Science* 262: 1422–25
14. Betzig E, Trautman JK. 1992. Near-field optics: microscopy, spectroscopy, and surface modification beyond the diffraction limit. *Science* 257:189–95
15. Bobroff N. 1986. Position measurement with a noise-limited instrument. *Rev. Sci. Instrum.* 57:1152–57
16. Bonnet G, Krichevsky O, Libchaber A. 1998. Kinetics of conformal fluctuations in DNA hairpin loops. *Proc. Natl. Acad. Sci. USA* 95:8602–6
17. Brasselet S, Moerner WE. 2000. Fluorescence behavior of single-molecule pH-sensors. *Single Mol.* 1:17–23
18. Carrington WA, Lynch RM, Moore EDW, Isenberg G, Fogarty KE, Fay FS. 1995. Superresolution three-dimensional images of fluorescence in cells with minimal light exposure. *Science* 268:1483–87
19. Chen Y, Muller JD, Tetin SY, Tyner JD, Gratton E. 2000. Probing ligand protein binding equilibria with fluorescence fluctuation spectroscopy. *Biophys. J.* 79: 1074–84

20. Corrie JE, Brandmeier BD, Ferguson RE, Trentham DR, Kendrick-Jones J, et al. 1999. Dynamic measurement of myosin light-chain-domain tilt and twist in muscle contraction. *Nature* 400:425–30
21. Cotton GJ, Muir TW. 1999. Peptide ligation and its application to protein engineering. *Chem. Biol.* 6:R247–56
22. Dahan M, Laurence T, Pinaud F, Chemla DS, Alivisatos AP, et al. 2001. Time-gated biological imaging using colloidal quantum dots. *Opt. Lett.* 26:825–28
23. Damjanovich S, Vereb G, Schaper A, Jenei A, Matko J, et al. 1995. Structural hierarchy in the clustering of HLA class I molecules in the plasma membrane of human lymphoblastoid cells. *Proc. Natl. Acad. Sci. USA* 92:1122–26
24. Dawson PE, Kent SB. 2000. Synthesis of native proteins by chemical ligation. *Annu. Rev. Biochem.* 69:923–60
25. de Lange F, Cambi A, Huijbens R, de Bakker B, Rensen W, et al. 2001. Cell biology beyond the diffraction limit: near-field scanning optical microscopy. *J. Cell Sci.* 114:4153–60
26. Deniz AA, Dahan M, Grunwell JR, Ha T, Faulhaber AE, et al. 1999. Single-pair fluorescence resonance energy transfer on freely diffusing molecules: observation of Förster distance dependence and subpopulations. *Proc. Natl. Acad. Sci. USA* 96:3670–75
27. Deniz AA, Laurence TA, Beligere GS, Dahan M, Martin AB, et al. 2000. Single-molecule protein folding: diffusion fluorescence resonance energy transfer studies of the denaturation of chymotrypsin inhibitor 2. *Proc. Natl. Acad. Sci. USA* 97:5179–84
28. Denk W, Strickler JH, Webb WW. 1990. Two-photon laser scanning fluorescence microscopy. *Science* 248:73–76
29. Deschenes LA, Vanden Bout DA. 2001. Single-molecule studies of heterogeneous dynamics in polymer melts near the glass transition. *Science* 292:255–58
30. Dickinson ME, Bearman G, Tille S, Lansford R, Fraser SE. 2001. Multi-spectral imaging and linear unmixing add a whole new dimension to laser scanning fluorescence microscopy. *Biotechniques* 31: 1272–78
31. Dickson RM, Cubitt AB, Tsien RY, Moerner WE. 1997. On/off blinking and switching behaviour of single molecules of green fluorescent protein. *Nature* 388: 355–58
32. Dittrich PS, Schwille P. 2001. Photobleaching and stabilization of fluorophores used for single-molecule analysis with one- and two-photon excitation. *Appl. Phys. B* 73:829–37
33. Dyba M, Hell SW. 2002. Focal spot of size $\lambda/23$ open up far-field fluorescence microscopy at 33 nm axial resolution. *Phys. Rev. Lett.* 88:163901–4
34. Efron B, Tibshirani R. 1993. *An Introduction to the Bootstrap*. New York: Chapman & Hall. 436 pp.
35. Efros AL, Rosen M. 1997. Random telegraph signal in the photoluminescence intensity of a single quantum dot. *Phys. Rev. Lett.* 78:1110–13
36. Elson EL, Magde D. 1974. Fluorescence correlation spectroscopy. I. Conceptual basis and theory. *Biopolymers* 13:1–27
37. Empedocles SA, Norris DJ, Bawendi MG. 1996. Photoluminescence spectroscopy of single CdSe nanocrystallite quantum dots. *Phys. Rev. Lett.* 77:3873–76
38. Enderle T, Ha T, Ogletree DF, Chemla DS, Magowan C, Weiss S. 1997. Membrane specific mapping and colocalization of malarial and host skeletal proteins in the *Plasmodium falciparum* infected erythrocyte by dual-color near-field scanning optical microscopy. *Proc. Natl. Acad. Sci. USA* 94:520–25
39. Forkey JN, Quinlan ME, Goldman YE. 2000. Protein structural dynamics by single-molecule fluorescence polarization. *Prog. Biophys. Mol. Biol.* 74:1–35
40. Förster. 1948. Zwischenmolekulare Energiewanderung und Fluoreszenz. *Ann. Physik* 6:55–75

41. Frohn JT, Knapp HF, Stemmer A. 2000. True optical resolution beyond the Rayleigh limit achieved by standing wave illumination. *Proc. Natl. Acad. Sci. USA* 97: 7232–36
42. Funatsu T, Harada Y, Tokunaga M, Saito K, Yanagida T. 1995. Imaging of single fluorescent molecules and individual ATP turnovers by single myosin molecules in aqueous solution. *Nature* 374:555–59
43. Gadella TW Jr, van der Krogt GN, Bisseling T. 1999. GFP-based FRET microscopy in living plant cells. *Trends Plant Sci.* 4:287–91
44. Gadella TWJ, Jovin TM. 1995. Oligomerization of epidermal growth factor receptors on A431 cells studied by time-resolved fluorescence imaging microscopy—a stereochemical model for tyrosine kinase receptor activation. *J. Cell. Biol.* 129:1543–58
45. Gadella TWJ, Jovin TM, Clegg RM. 1993. Fluorescence lifetime imaging microscopy (FLIM)—spatial resolution of microstructures on the nanosecond time scale. *Biophys. Chem.* 48:221–39
46. Gelles J, Schnapp BJ, Sheetz MP. 1988. Tracking kinesin-driven movements with nanometer-scale precision. *Nature* 331: 450–53
47. Goulian M, Simon SM. 2000. Tracking single proteins within cells. *Biophys. J.* 79:2188–98
48. Griffin BA, Adams SR, Tsien RY. 1998. Specific covalent labeling of recombinant protein molecules inside live cells. *Science* 281:269–72
49. Grinvald A, Haas E, Steinberg IZ. 1972. Evaluation of the distribution of distances between energy donors and acceptors by fluorescence decay. *Proc. Natl. Acad. Sci. USA* 69:2273–77
50. Gustafsson MGL, Agard DA, Sedat JW. 1999. ISM: 3D widefield light microscopy with better than 100 nm axial resolution. *J. Microsc.* 195:10–16
51. Ha T, Enderle T, Chemla DS, Selvin PR, Weiss S. 1996. Single molecule dynamics studied by polarization modulation. *Phys. Rev. Lett.* 77:3979–82
52. Ha T, Enderle T, Chemla DS, Selvin PR, Weiss S. 1997. Quantum jumps of single molecules at room temperature. *Chem. Phys. Lett.* 271:1–5
53. Ha T, Enderle T, Chemla DS, Weiss S. 1996. Dual-molecule spectroscopy: molecular rulers for the study of biological macromolecules. *IEEE J. Sel. Top. Quant. Elec.* 2:1115–28
54. Ha T, Glass J, Enderle T, Chemla DS, Weiss S. 1998. Hindered rotational diffusion and rotational jumps of single molecules. *Phys. Rev. Lett.* 80:2093–96
55. Ha T, Laurence TA, Chemla DS, Weiss S. 1999. Polarization spectroscopy of single fluorescent molecules. *J. Phys. Chem. B* 103:6839–50
56. Ha T, Ting AY, Liang J, Caldwell WB, Deniz AA, et al. 1999. Single-molecule fluorescence spectroscopy of enzyme conformational dynamics and cleavage mechanism. *Proc. Natl. Acad. Sci. USA* 96:893–98
57. Hanley QS, Arndt-Jovin DJ, Jovin TM. 2002. Spectrally resolved fluorescence lifetime imaging microscopy. *Appl. Spectrosc.* 56:155–66
58. Harms GS, Cognet L, Lommerse PHM, Blab GA, Kahr H, et al. 2001. Single-molecule imaging of L-type Ca²⁺ channels in live cells. *Biophys. J.* 81:2639–46
59. Haugland RP. 2002. *Handbook of Fluorescent Probes and Research Products*. Eugene, OR: Molecular Probes. 966 pp.
60. Hell S, Stelzer EHK. 1992. Properties of a 4Pi confocal fluorescence microscope. *J. Opt. Soc. Am. A* 9:2159–66
61. Hiraoka Y, Sedat JW, Agard DA. 1987. The use of charge-coupled device for quantitative optical microscopy of biological structures. *Science* 238:36–41
62. Hofkens J, Schroyers W, Loos D, Cotlet M, Köhn F, et al. 2001. Triplet states as

- non-radiative traps in multichromophoric entities: single molecule spectroscopy of an artificial and natural antenna system. *Spectrosc. Acta A* 57:2093–107
63. Iino R, Koyama I, Kusumi A. 2001. Single molecule imaging of green fluorescent proteins in living cells: E-cadherin forms oligomers on the free cell surface. *Bio-phys. J.* 80:2667–77
64. Ishijima A, Yanagida T. 2001. Single molecule nanobioscience. *Trends Biochem. Sci.* 26:438–44
65. Jia Y, Talaga D, Lau W, Lu H, DeGrado W, Hochstrasser R. 1999. Folding dynamics of single GCN4 peptides by fluorescence resonant energy transfer confocal microscopy. *Chem. Phys.* 247:69–83
66. Kapanidis AN, Weiss S. 2002. Fluorescent probes and bioconjugation chemistries for single-molecule fluorescence analysis of biomolecules. *J. Chem. Phys.* 117(24):10953–64
67. Klar TA, Jakobs S, Dyba M, Egner A, Hell SW. 2000. Fluorescence microscopy with diffraction resolution barrier broken by stimulated emission. *Proc. Natl. Acad. Sci. USA* 97:8206–10
68. Kunkel TA, Bebenek K, McClary J. 1991. Efficient site-directed mutagenesis using uracil-containing DNA. *Methods Enzymol.* 204:125–39
69. Lacoste TD, Michalet X, Pinaud F, Chemla DS, Alivisatos AP, Weiss S. 2000. Ultrahigh-resolution multicolor colocalization of single fluorescent probes. *Proc. Natl. Acad. Sci. USA* 97:9461–66
70. Lakowicz JR. 1999. *Principles of Fluorescence Spectroscopy*. New York: Plenum. 698 pp.
71. Lakowicz JR, Berndt KW. 1991. Lifetime-selective fluorescence imaging using an RF phase-sensitive camera. *Rev. Sci. Instrum.* 62:1727–34
72. Lakowicz JR, Szymanski H, Nowaczyk K, Lederer WJ, Kirby MS, Johnson ML. 1994. Fluorescence lifetime imaging of intracellular calcium in COS cells using quin-2. *Cell Calcium* 15:7–27
73. Lu HP, Xun L, Xie XS. 1998. Single-molecule enzymatic dynamics. *Science* 282:1877–82
74. Mackay CD, Tubbs RN, Bell R, Burt D, Jerram P, Moody I. 2001. Sub-electron read noise at MHz pixel rates. *SPIE Proc.* 4306:289–98
75. Macklin JJ, Trautman JK, Harris TD, Brus LE. 1996. Imaging and time-resolved spectroscopy of single molecules at an interface. *Science* 272:255–58
76. Magde D, Elson EL, Webb WW. 1974. Fluorescence correlation spectroscopy. II. An experimental realization. *Biopolymers* 13:29–61
77. Mainen ZF, Maletic-Savatic M, Shi SH, Hayashi Y, Malinow R, Svoboda K. 1999. Two-photon imaging in living brain slices. *Methods* 18:231–39
78. Malik Z, Cabib D, Buckwald RA, Talmi A, Garini Y, Lipson SG. 1996. Fourier transform multipixel spectroscopy for quantitative cytology. *J. Microsc.* 182:133–40
79. Margeat E, Poujol N, Boulahtouf A, Chen Y, Muller JD, et al. 2001. The human estrogen receptor alpha dimer binds a single SRC-1 coactivator molecule with an affinity dictated by agonist structure. *J. Mol. Biol.* 306:433–42
80. Mekler V, Kortkhonja E, Mukhopadhyay J, Knight J, Revyakin A, et al. 2002. Structural organization of RNA polymerase holoenzyme and the RNA polymerase-promoter open complex: systematic fluorescence resonance energy transfer and distance-constrained docking. *Cell* 108:1–20
81. Michalet X, Lacoste TD, Weiss S. 2001. Ultrahigh-resolution colocalization of spectrally resolvable point-like fluorescent probes. *Methods* 25:87–102
82. Michalet X, Pinaud F, Lacoste TD, Dahan M, Bruchez MP, et al. 2001. Properties of fluorescent semiconductor nanocrystals and their application to biological labeling. *Single Mol.* 2:261–76

83. Michalet X, Weiss S. 2002. Single-molecule spectroscopy and microscopy. *C. R. Phys.* 3:619–44
84. Moerner WE. 1994. Examining nanoenvironments in solids on the scale of a single, isolated impurity molecule. *Science* 265:46–53
85. Moerner WE. 2002. A dozen years of single-molecule spectroscopy in physics, chemistry, and biophysics. *J. Phys. Chem. B* 106:910–27
86. Moerner WE, Kador L. 1989. Optical detection and spectroscopy of single molecules in a solid. *Phys. Rev. Lett.* 62:2535–38
87. Moerner WE, Orrit M. 1999. Illuminating single molecules in condensed matter. *Science* 283:1670–76
88. Muir TW, Sondhi D, Cole PA. 1998. Expressed protein ligation: a general method for protein engineering. *Proc. Natl. Acad. Sci. USA* 95:6705–10
89. Mukhopadhyay J, Kapanidis AN, Mekler V, Kortkhonjia E, Ebright YW, Ebright RH. 2001. Translocation of S70 with RNA polymerase during transcription: fluorescence resonance energy transfer assay for movement relative to DNA. *Cell* 106:453–63
90. Nemoto N, Miyamoto-Sato E, Yanagawa H. 1999. Fluorescence labeling of the C-terminus of proteins with a puromycin analogue in cell-free translation systems. *FEBS Lett.* 462:43–46
91. Neuhauser RG, Shimizu KT, Woo WK, Empedocles SA, Bawendi MG. 2000. Correlation between fluorescence intermittency and spectral diffusion in single semiconductor quantum dots. *Phys. Rev. Lett.* 85:3301–4
92. Ng T, Squire A, Hansra G, Bornancin F, Prevostel C, et al. 1999. Imaging protein kinase C α activation in cells. *Science* 283:2085–89
93. Nirmal M, Dabbousi BO, Bawendi MG, Macklin JJ, Trautman JK, et al. 1996. Fluorescence intermittency in single cadmium selenide nanocrystals. *Nature* 383:802–4
94. Nishiyama M, Muto E, Inoue Y, Yanagida T, Higuchi H. 2001. Substeps within the 8-nm step of the ATPase cycle of single kinesin molecules. *Nat. Cell Biol.* 3:425–28
95. Orrit M, Bernard J. 1990. Single pentacene molecules detected by fluorescence excitation in a *p*-terphenyl crystal. *Phys. Rev. Lett.* 65:2716–19
96. Patterson GH, Piston DW. 2000. Photo-bleaching in two-photon excitation microscopy. *Biophys. J.* 78:2159–62
97. Pawley JB, ed. 1995. *Handbook of Biological Confocal Microscopy*. New York: Plenum
98. Pepperkok R, Squire A, Geley S, Bastiaens PIH. 1999. Simultaneous detection of multiple green fluorescent proteins in live cell by fluorescent lifetime imaging microscopy. *Curr. Biol.* 9:269–72
99. Perrin F. 1929. La fluorescence des solutions. *Ann. Phys.* 12:169–275
100. Perrin F. 1932. Théorie quantique des transferts d'activation entre molécules de même espèce. Cas des solutions fluorescentes. *Ann. Phys.* 17:283–313
101. Peterman EJ, Sosa H, Goldstein LS, Moerner WE. 2001. Polarized fluorescence microscopy of individual and many kinesin motors bound to axonemal microtubules. *Biophys. J.* 81:2851–63
102. Piston DW, Sandison DR, Webb WW. 1992. Time-resolved fluorescence imaging and background rejection by two-photon excitation in laser scanning microscopy. *Proc. SPIE* 1640:379–89
103. Rarbach M, Kettling U, Koltermann A, Eigen M. 2001. Dual-color fluorescence cross-correlation spectroscopy for monitoring the kinetics of enzyme-catalyzed reactions. *Methods* 24:104–16
104. Rudiger M, Haupts U, Moore KJ, Pope AJ. 2001. Single-molecule detection technologies in miniaturized high throughput screening: binding assays for G protein-coupled receptors using fluorescence

- intensity distribution analysis and fluorescence anisotropy. *J. Biomol. Screen.* 6:29–37
105. Sako Y, Minoguchi S, Yanagida T. 2000. Single-molecule imaging of EGFR signalling on the surface of living cells. *Nat. Cell Biol.* 2:168–72
 106. Sánchez EJ, Novotny L, Holtom GR, Xie SX. 1997. Room-temperature fluorescence imaging and spectroscopy of single molecules by two-photon excitation. *J. Phys. Chem. A* 101:7019–23
 107. Sase I, Miyata H, Ishiwata S, Kinoshita K Jr. 1997. Axial rotation of sliding actin filaments revealed by single-fluorophore imaging. *Proc. Natl. Acad. Sci. USA* 94:5646–50
 108. Scheel AA, Funsch B, Busch M, Gradl G, Pschorr J, Lohse MJ. 2001. Receptor-ligand interactions studied with homogeneous fluorescence-based assays suitable for miniaturized screening. *J. Biomol. Screen.* 6:11–18
 109. Schmidt T, Schütz GJ, Baumgartner W, Gruber HJ, Schindler H. 1996. Imaging of single molecule diffusion. *Proc. Natl. Acad. Sci. USA* 93:2926–29
 110. Schütz GJ, Pastushenko VP, Gruber H, Knaus H-G, Pragl B, Schindler H. 2000. 3D imaging of individual ion channels in live cells at 40 nm resolution. *Single Mol.* 1:25–31
 111. Schwille P. 2001. Fluorescence correlation spectroscopy and its potential for intracellular applications. *Cell Biochem. Biophys.* 34:383–408
 112. Selvin PR. 1995. Fluorescence resonance energy transfer. *Methods Enzymol.* 246:300–34
 113. Severinov K, Muir TW. 1998. Expressed protein ligation, a novel method for studying protein-protein interactions in transcription. *J. Biol. Chem.* 273:16205–9
 114. So PT, Dong CY, Masters BR, Berland KM. 2000. Two-photon excitation fluorescence microscopy. *Annu. Rev. Biomed. Eng.* 2:399–429
 115. So PTC, French T, Yu WM, Berland KM, Dong CY, Gratton E. 1995. Time-resolved fluorescence microscopy using two-photon excitation. *Bioimaging* 3:49–63
 116. Sosa H, Peterman EJG, Moerner WE, Goldstein SB. 2001. ADP-induced rocking of the kinesin motor domain revealed by single-molecule fluorescence polarization microscopy. *Nat. Struct. Biol.* 8:540–44
 117. Straub M, Hell SW. 1998. Fluorescence lifetime three-dimensional microscopy with picosecond precision using a multifocal multiphoton microscope. *Appl. Phys. Lett.* 73:1769–71
 118. Stryer L, Haugland RP. 1967. Energy transfer: a spectroscopic ruler. *Proc. Natl. Acad. Sci. USA* 58:719–26
 119. Syngé EH. 1928. A suggested method for extending microscopic resolution into the ultra-microscopic region. *Philos. Mag.* 6:356–62
 120. Sytsma J, Vroom JM, DeGrauw CJ, Gerritsen HC. 1998. Time-gated fluorescence lifetime imaging and microvolume spectroscopy using two-photon excitation. *J. Microsc.* 191:39–51
 121. Taguchi H, Ueno T, Tadakuma H, Yoshida M, Funatsu T. 2001. Single-molecule observation of protein-protein interactions in the chaperonin system. *Nat. Biotechnol.* 19:861–65
 122. Tam JP, Xu J, Eom KD. 2001. Methods and strategies of peptide ligation. *Biopolymers* 60:194–205
 123. Terpetschnig E, Szmecinski H, Malak H, Lakowicz JR. 1995. Metal-ligand complexes as a new class of long-lived fluorophores for protein hydrodynamics. *Bioophys. J.* 68:342–50
 124. Tinnefeld P, Buschmann V, Herten D-P, Han K-T, Sauer M. 2000. Confocal fluorescence lifetime imaging microscopy (FLIM) at the single molecule level. *Single Mol.* 1:215–23
 125. Trautman JK, Macklin JJ, Brus LE, Betzig E. 1994. Near-field spectroscopy of single

- molecules at room temperature. *Science* 369:40–42
126. Tsien RY. 1998. The green fluorescent protein. *Annu. Rev. Biochem.* 67:509–44
 127. Vale RD, Funatsu T, Pierce DW, Romberg L, Harada Y, Yanagida T. 1996. Direct observation of single kinesin molecules moving along microtubules. *Nature* 380: 451–53
 128. van Oijen AM, Köhler J, Schmidt J, Müller M, Brakenhoff GJ. 1998. 3-Dimensional super-resolution by spectrally selective imaging. *Chem. Phys. Lett.* 292:183–87
 129. Van Rompaey E, Chen Y, Muller JD, Gratton E, Van Craenenbroeck E, et al. 2001. Fluorescence fluctuation analysis for the study of interactions between oligonucleotides and polycationic polymers. *Biol. Chem.* 382:379–86
 130. Vanden Bout DA, Yip W-T, Hu D, Fu D-K, Swager TM, Barbara PF. 1997. Discrete intensity jumps and intramolecular electronic energy transfer in the spectroscopy of single conjugated polymer molecules. *Science* 277:1074–77
 131. Vereb G, Jares-Erijman E, Selvin PR, Jovin TM. 1998. Temporally and spectrally resolved imaging microscopy of lanthanide chelates. *Biophys. J.* 74:2210–22
 132. Waggoner A. 1995. Covalent labeling of proteins and nucleic acids with fluorophores. *Methods Enzymol.* 246:362–73
 133. Wang Y-L, Taylor DL, eds. 1989. *Fluorescence Microscopy of Living Cells in Culture. Part A & B.* San Diego: Academic. Vols. 29, 30
 134. Wang XF, Periasamy A, Herman B. 1992. Fluorescence lifetime imaging microscopy (FLIM): instrumentation and applications. *Crit. Rev. Anal. Chem.* 23: 369–95
 135. Warshaw DM, Hayes E, Gaffney D, Lauzon AM, Wu J, et al. 1998. Myosin conformational states determined by single fluorophore polarization. *Proc. Natl. Acad. Sci. USA* 95:8034–39
 136. Weiss S. 1999. Fluorescence spectroscopy of single biomolecules. *Science* 283:1676–83
 137. Weiss S. 2000. Measuring conformational dynamics of biomolecules by single molecule fluorescence spectroscopy. *Nat. Struct. Biol.* 7:724–29
 138. Widengren J, Mets U, Rigler R. 1995. Fluorescence correlation spectroscopy of triplet states in solution—a theoretical and experimental study. *J. Phys. Chem.* 99:13368–79
 139. Widengren J, Rigler R. 1998. Fluorescence correlation spectroscopy as a tool to investigate chemical reactions in solutions and on cell surfaces. *Cell. Mol. Biol.* 44:857–79
 140. Wu M, Goodwin PM, Ambrose WP, Keller RA. 1996. Photochemistry and fluorescence emission dynamics of single molecules in solution-B-phycoerythrin. *J. Phys. Chem.* 100:17406–9
 141. Xie XS, Dunn RC. 1994. Probing single molecule dynamics. *Science* 265:361–64
 142. Xie XS, Trautman JK. 1998. Optical studies of single molecules at room temperature. *Annu. Rev. Phys. Chem.* 49:441–80
 143. Yamaguchi J, Nemoto N, Sasaki T, Tokumasu A, Mimori-Kiyosue Y, et al. 2001. Rapid functional analysis of protein-protein interactions by fluorescent C-terminal labeling and single-molecule imaging. *FEBS Lett.* 502:79–83
 144. Yasuda R, Noji H, Yoshida M, Kinoshita K, Itoh H. 2001. Resolution of distinct rotational substeps by submillisecond kinetic analysis of F₁-ATPase. *Nature* 410:898–904
 145. Zhuang X, Bartley LE, Babcock HP, Russell R, Ha T, et al. 2000. A single-molecule study of RNA catalysis and folding. *Science* 288:2048–51

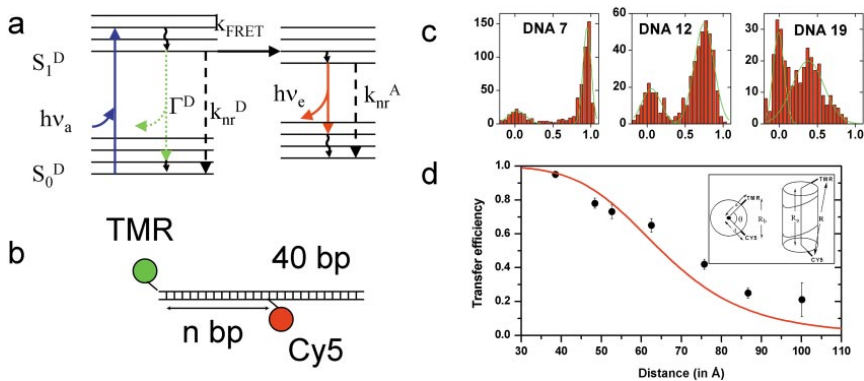


Figure 3 (a) Jablonski diagram for FRET. Fluorescence energy transfer involves two molecules: a donor D and an acceptor A, whose absorption spectrum overlaps the emission spectrum of the donor. Excitation of the acceptor to the lowest singlet excited state is a process identical to that described for single-molecule fluorescence (Figure 1). Energy transfer to the acceptor by dipole-dipole interaction, in the presence (within a few nm) of a nearby acceptor molecule, quenches donor fluorescence emission. The donor exhibits fluorescent emission following the rules outlined in Figure 1a. (b) DNA n constructs used for the FRET distance study. Tetramethylrhodamine (TMR) is attached to the 5' end of the DNA, and Cy5 is attached to the n^{th} base from the 5' end ($n = 7, 12, 14, 16, 19, 24, 27$). (c) FRET histograms extracted from time traces for DNA 7, 12, and 19. Double Gaussian fits extract numbers for the mean (width) of the higher efficiency peak of 0.95 ± 0.05 , 0.75 ± 0.13 , and 0.38 ± 0.21 , respectively. The peak around zero efficiency corresponds to nonfluorescent acceptor molecules. (d) Mean FRET efficiencies extracted from FRET histograms plotted as a function of distance for DNA 7, 12, 14, 16, 19, 24, and 27. Distances are calculated using the known B-DNA double-helix structure. The solid line corresponds to the expected Förster transfer curve for $R_0 = 65 \text{ \AA}$. (b, c) Adapted with permission from Reference 26. Copyright 1999, the National Academy of Sciences USA.

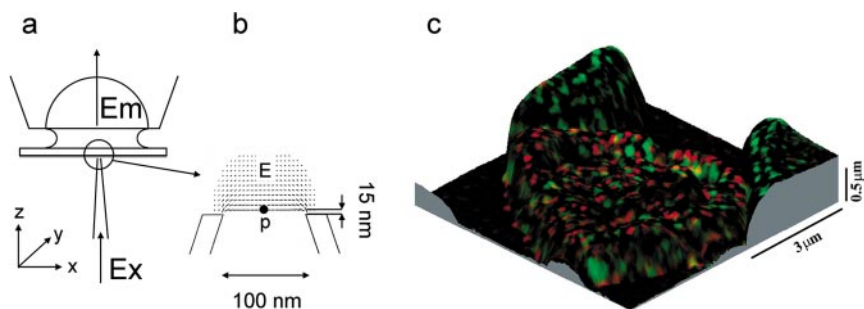


Figure 4 (a) Schematic of a near-field scanning optical microscope setup used for single-molecule imaging. An aluminum-coated tapered optical fiber (raster-scanned at nanometer distance from the sample) with a subwavelength aperture (50–100 nm) serves as a waveguide for laser excitation. Shear-force feedback keeps the tip at a constant distance from the sample, resulting in a signal used for nanometer-resolution topographic reconstruction of the scanned area. (b) The excitation volume and the corresponding local evanescent electric field are detailed in the expanded view. Fluorescence light emitted by individual molecules is collected by an oil immersion, high NA objective and recorded by an APD. (c) Composite image obtained by superimposing the fluorescence intensity detected in two separate channels over a topographic map of red blood cells obtained by shear force feedback of the near-field microscope. Green spots correspond to fluorescence of host proteins labeled with FITC. Red spots correspond to malaria proteins labeled with Texas Red. (a, b) Adapted with permission from Reference 13. Copyright 1993, the American Association for the Advancement of Science. (c) Adapted with permission from Reference 53. Copyright 1996, IEEE.

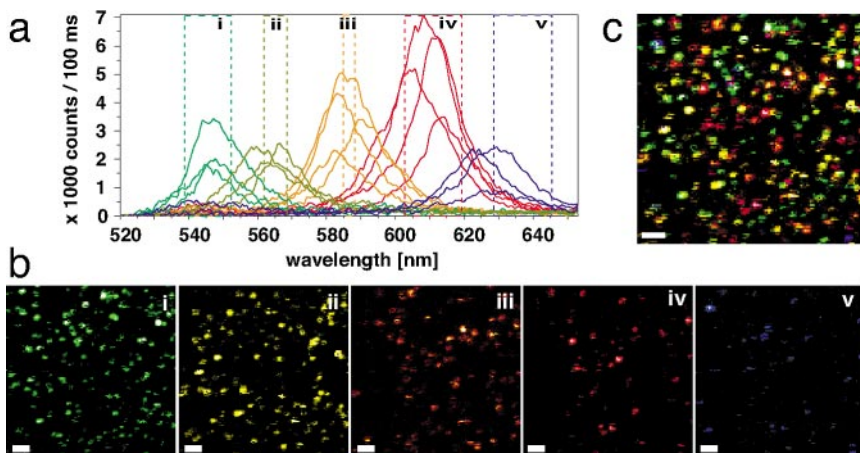


Figure 5 Spectral imaging semiconductor nanocrystals. Scans of a mixture of four NC samples (ensemble peak emissions: 540, 575, 588, and 620 nm). (a) A representative collection of individual NC spectra (about 20 nm FWHM) obtained from the integrated data of 3×3 pixels. Despite their overlap, five orthogonal spectral bands (*i* to *v*) could be defined. (b) Five false-color images corresponding to the spectral bands defined in (a). (c) Overlay of the five perfectly registered images of (b). $10 \times 10 \mu\text{m}^2$ scan (pixel size: 78 nm, scale bar: $1 \mu\text{m}$). Adapted with permission from Reference 81. Copyright 2001, Academic Press.

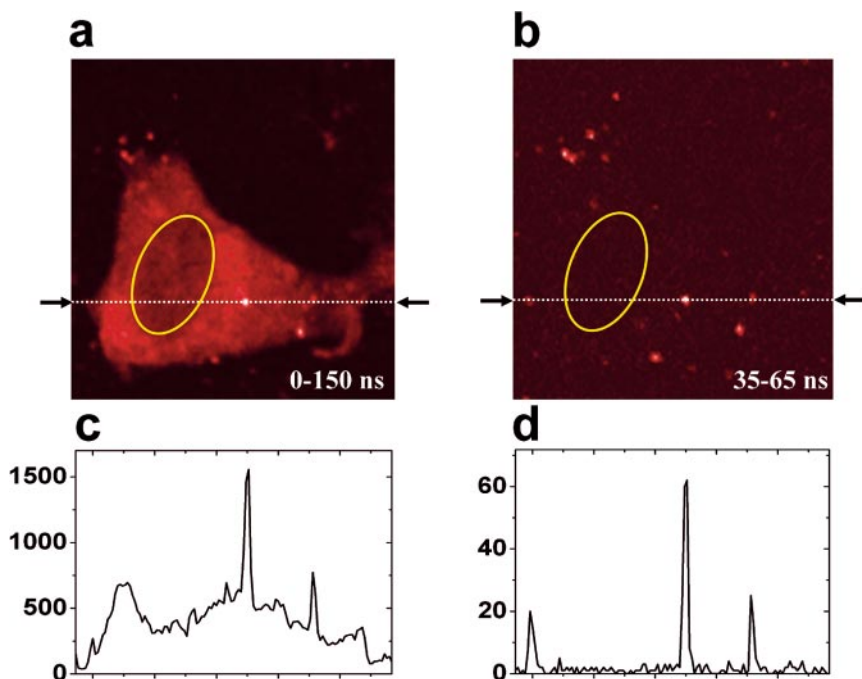


Figure 6 (right) Time-gated imaging of semiconductor NCs. (a) Mouse 3T3 fibroplasts were incubated with NCs and fixed in 2% formaldehyde, 0.5% glutaraldehyde. Observations were performed using a customized confocal microscope [for details see (22)]. Integration time per pixel is 10 ms, the lifetime window being 0–150 ns after the laser pulse (repetition rate: 5 MHz). This image is obtained using all the detected photons. The ellipse indicates the location of the nucleus. (b) The same recording, but retaining only photons arrived between 35 and 65 ns after a laser pulse. A marked decrease of the background is observed with a few bright spots clearly dominating. (c, d) Intensity profiles along the white-dashed line in a and b. The total signal decreases notably, but the signal-to-average-background ratio jumps from 3 to 45. Note that part of the cytoplasm fluorescence might also be due to NCs. Adapted with permission from Reference 22. Copyright 2001, Optical Society of America.

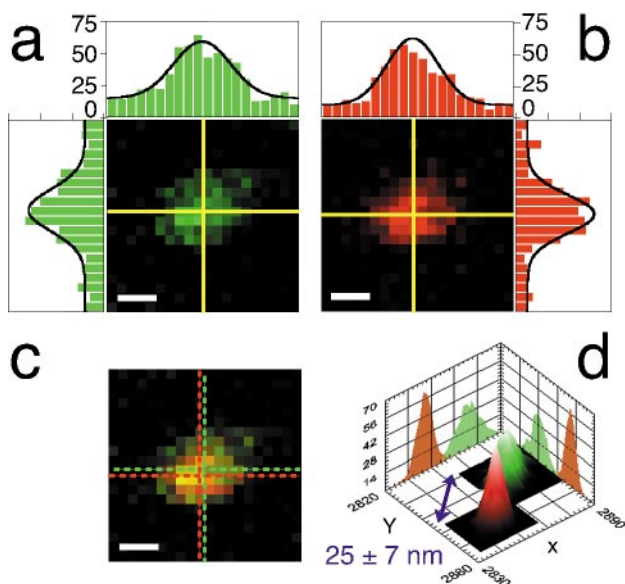


Figure 7 Ultrahigh-resolution colocalization of individual nanocrystals. Mixture of green (Em: 540 nm) and red (Em: 620 nm) NCs excited at 488 nm (excitation power: 200 nW incident or 320 W/cm² peak irradiance; integration time: 50 ms). (a, b) Green and red channel images of a $1 \times 1 \mu\text{m}^2$ scan obtained by raster scanning the sample through the fixed excitation PSF and recording the respective signals on two different APDs (pixel size: 50 nm; scale bar: 200 nm). As visible from the intensity profiles along two orthogonal lines passing through the PSFs centers, the count rates are similar in both channels. Black curves indicate the corresponding cross-sections of the fitted PSFs. (c) Overlay of the two channels with indication of the determined PSFs centers. (d) Bootstrap replicas of the datasets were fitted in order to estimate the uncertainty of the position determination (34). The figure shows the histograms of the fitted centers distribution obtained from 1000 simulations. The measured distance is 25 nm with a corresponding uncertainty of 7 nm (68% confidence limit). Adapted with permission from Reference 69. Copyright 2000, the National Academy of Sciences USA.